Sustainable Food Technology

ROYAL SOCIETY OF CHEMISTRY

PAPER

View Article Online
View Journal | View Issue

Cite this: *Sustainable Food Technol.*, 2025, **3**, 1492

Enhanced stability of n-3 PUFAs rich structured lipids *via* spray-dried microencapsulation with tailored wall materials

Mudassar Hussain, [a] Abhishek Bisht, [b] Imad Khan,[a] Muneeba Naseer Chaudhary,[c] Nida Kanwal,[a] Muhammad Umair Khalid,[a] Mst Nushrat Yiasmin,[a] Arif Hussain[a] and Xiaoqiang Zou*[a]

This study aimed to develop and evaluate the microencapsulation of n-3 PUFAs-rich medium- and long-chain structured lipids (MLSLs) using gum arabic (GA), maltodextrin (MD), and modified starch (MS) in various ratios. Microcapsules were produced *via* spray drying and assessed for microencapsulation yield, microencapsulation efficiency, physicochemical characteristics, and oxidative stability. The GA:MS:MD formulation achieved the highest microencapsulation yield (87.77 ± 0.47% w/w) and microencapsulation efficiency (90.11 ± 0.56% w/w), with optimal moisture content (1.98 ± 0.21% w/w), water activity (0.17 ± 0.04), and superior wettability (9.27 ± 0.72 min). It also exhibited enhanced solubility (87.54 ± 0.63% w/w) and a low polydispersity index (PDI) (0.28 ± 0.03). FT-IR confirmed successful encapsulation, SEM revealed intact spherical microcapsules, and peroxide values under accelerated storage (55 °C, 28 days) remained low (0.71–2.39 meq O_2 per kg). These findings highlight GA:MS:MD microcapsules as promising candidates for functional food and pharmaceutical applications.

Received 6th May 2025
Accepted 18th July 2025

DOI: 10.1039/d5fb00185d

rsc.li/susfoodtech

Sustainability spotlight

This study presents an innovative approach to enhance the oxidative stability and shelf-life of n-3 PUFAs-rich structured lipids through microencapsulation using bio-degradable and food-grade wall materials. By optimizing spray-drying techniques with gum arabic, maltodextrin, and modified starch, the process supports clean-label formulation and reduce reliance on synthetic antioxidants. The encapsulated lipids offer potential for inclusion in functional foods, minimizing wastage of high-value oils and improving nutritional delivery. This contributes to sustainable food systems through improved ingredients preservation, reduced spoilage, and enhanced product stability.

1 Introduction

Sustainable microencapsulation has emerged as a key technology in recent years due to its role in enhancing stability, bioavailability, and functionality of bioactive compounds while promoting environmental sustainability and aligning with global goals such as the United Nations Sustainable Development Goal (SDG) 12: Responsible Consumption and Production.[1] This process involves encapsulating active ingredients such as oils, phenolic compounds, and bioactives to protect them from environmental degradation and ensure their controlled release. For instance, phenolic compounds have been extensively encapsulated *via* spray drying from natural sources like ciriguela peel, achieving high improved stability and encapsulation effectiveness during storage.[2] Similarly, innovative materials such as sporopollenin microcapsules have shown promise as delivery systems for bioactives, combining degradability, photoprotective properties, and minimal environmental impact, reinforcing their suitability for sustainable applications.[3] The use of biodegradable and food-grade wall materials such as maltodextrin (MD), gum arabic (GA), and octenyl succinic anhydride (OSA) modified starches (MS) in microencapsulation processes further contributes to sustainability by reducing reliance on synthetic polymers and promoting eco-friendly product development.[4] These advancements underscore the importance of sustainable encapsulation techniques in pharmaceuticals, food, and cosmetic industries.

In recent years, there has been increasing interest in synthesizing medium- and long-chain structured lipids (MLSLs)

[a]*State Key Laboratory of Food Science and Resources, National Engineering Research Center for Functional Food, National Engineering Research Center of Cereal Fermentation and Food Biomanufacturing, Collaborative Innovation Center of Food Safety and Quality Control in Jiangsu Province, School of Food Science and Technology, Jiangnan University, 1800 Lihu Road, Binhu District, Wuxi 214122, Jiangsu, China. E-mail: xiaoqiangzou@163.com*

[b]*Department of Food Technology, School of Allied Sciences, Dev Bhoomi Uttarakhand University, Navgaon, Manduwala, Chakrata Road, Dehradun 248007, Uttarakhand, India*

[c]*Integrative Science Center of Germplasm Creation in Western China (CHONGQING) Science City/College of Food Science, Southwest University, Chongqing, 400715, China*

through enzymatic reactions using lipases as catalysts. Long-chain fatty acids (LCFAs) are metabolized slowly and tend to accumulate in human adipose tissue.[5] In contrast, medium-chain fatty acids (MCFAs) are rapidly metabolized and serve as quick source of energy. Unlike LCFAs, MCFAs are transported directly to the liver *via* the portal vein rather than through the lymphatic system, reducing their likelihood of being stored as fat. Additionally, MCFAs possess antiviral and antibacterial properties, providing infants with protection against harmful microorganisms.[6] To mitigate the undesired effects of both LCFAs and MCFAs, the synthesis of MLSLs is essential.[7,8]

Moreover, these MLSLs are a unique form of oils with advantageous functional properties, such as easy absorption, low calories content, and minimal saturated fat. These lipids are synthesized by modifying the structure, composition, and distribution of fatty acids on the glycerol backbone of natural triacylglycerols (TAGs), which can influence fat digestion, stomach emptying rates, and metabolic responses.[9] To enhance enzymatic selectivity and yield during MLSL synthesis, we utilized a "bio-imprinting" approach on immobilized lipases, as demonstrated in our previous study.[8] This technique involves pre-conditioning the enzyme with substrate analogs or additives to induce conformational changes, thereby stabilizing its active form and improving catalytic efficiency—particularly in non-aqueous systems. The tailored structural features of MLSLs offer promising physiological and nutritional benefits, including reduced body fat accumulation, improved fat malabsorption, and decreased risk of obesity and cardiovascular diseases.[10] A key component in MLSL formulations, particularly from fish oil sources, are omega-3 polyunsaturated fatty acids (n-3 PUFAs) such as eicosapentaenoic acid (EPA, 20 : 5) and docosahexaenoic acid (DHA, 22 : 6). These essential fatty acids, which the human body synthesizes inefficiently, must be obtained through diet and have been widely associated with preventing or managing a variety of chronic conditions—including cardiovascular diseases, atherosclerosis, cancer, dyslipidemia, obesity, inflammatory, and neurological disorders, asthma and rheumatoid arthritis.[11] Despite these advantages, the utilization of these n-3 PUFAs-rich MLSLs are accompanied by certain challenges, including poor stability during oxidation and limited shelf-life of the products. These issues can be mitigated by converting liquid oils into powder form through microencapsulation, protecting unsaturated fatty acids against deterioration brought on by environmental elements including air, moisture, and light. Additionally, microencapsulation can mask undesirable odors and enhance the ultimate product's solubility and handling characteristics.[12,13]

The most frequently used technique for microencapsulation is spray drying for encapsulating fats and/or oils on a large scale due to its affordability and easily accessible equipment. Unlike other microencapsulation methods, spray drying is straightforward and operates continuously. Furthermore, it makes the finished product more chemically and microbiologically stable.[14,15] Studies have shown that the materials used for encapsulation affect several emulsion attributes, including stability, viscosity, droplet size, and other features including surface oil, particle size, density, morphology, and oxidative stability during the encapsulated goods' drying and storage processes.[16] Using bio-based and biodegradable MD as an additional wall substance offers numerous benefits, including affordability, flavor protection from oxidation, low viscosity at high solid concentrations, neutral flavor and fragrance, and ease of digestion for humans. However, MD has drawbacks such as poor emulsification properties and little preservation of volatile substances during the spray drying process.[17] To mitigate these shortcomings, MD is frequently used with additional wall materials. Furthermore, because of their oxygen barrier and emulsifying properties, food-grade, biodegradable OSA-MS have become great options for wall development, providing stability against environmental stressors including heat, pH, and ionic strength.[18] These carbs are approved as food additives by food authorities and are available in various forms with different degrees of polymerization and molecular weight.[19] Additionally, GA, a commonly used wall material is composed of D-glucuronic acid, L-rhamnose, D-galactose, L-arabinose, and around 2% protein, is typically utilized in the microencapsulation process through spray drying.[20] It combines with most oils to make stable emulsions.[21] Although GA is highly effective as wall material, its high cost and limited availability pose challenges for large-scale applications.[22] To address this, our study combines GA with more accessible materials like MS and MD, reducing dependance on GA while maintaining encapsulation performance and improving industrial feasibility.[23]

To align with sustainability goals and improve the use of n-3 PUFA-rich MLSLs in functional and nutritious foods, these lipids can be converted to powder and then encapsulated utilizing spray drying technique in food goods. Hence, this study investigates the development of a novel combination of GA, MD, and MS as wall materials for the microencapsulation of the n-3 PUFAs-rich MLSLs by spray drying, as well as to assess the encapsulated material's physicochemical properties and oxidative resistance n-3 PUFAs-rich MLSLs while being stored.

2 Materials & methods

2.1. Materials

The supplier of Omax 1812, a blend of anchovies and sardine oils, was Qingdao Keyuan Marine Biochemistry Co., Ltd. (Qingdao, Shandong, China) as a supply of LCFAs. The proportion of fatty acids in Omax 1812 has been analyzed in our earlier research.[8] Caprylic acid (CA) (99%, as source of MCFAs), lauric acid (98%), myristic acid (99%), palmitic acid (99%), stearic acid (98%), and oleic acid (99%); in addition, Tween 20, 40, 60 and 80 were purchased from Aladdin Co., Ltd (Shanghai, China). All these FAs and Tweens were used for the bio-imprinting of lipases in our previous study. Commercially immobilized lipases were bought from Novozymes (Beijing, China), namely Lipo 435 (from *Candida antarctica*), Lipo RM IM (from *Rhizomucor miehei*), Novo 40086 (from *Aspergillus oryzae*), and Lipo TL IM (from *Thermomyces lanuginosus*). Commercial MS namely Hi-cap100 (HCP) was purchased from National Starch (USA). Sinopharm (Chemical Reagent Co., Ltd., China) was the supplier of GA. China's Shyuanye Co., Ltd. supplied the MD. High purity and analytical grade other chemicals and

solvents were employed in this study for extraction and analysis. All studies were conducted using distilled water.

2.2. Production and purification of n-3 PUFAs-rich MLSLs

According to our earlier work, the optimal conditions that produced the maximum yield of n-3 PUFAs-rich MLSLs were chosen for the large-scale production of n-3 PUFAs-rich MLSLs.[8] With a substrate mole ratio of fish oil, the solvent-free acidolysis reaction was carried out in a 500 mL stirred batch reactor that was kept at 60 °C for 8 hours, CA at 1 : 4 (mol mol^{-1}), 6 wt% bio-imprinted Lipo RM IM quantity as a catalyst, and constant stirring at 600 rpm. To minimize light exposure, the reactor was covered with foil throughout the reaction. After completion, n-3 PUFAs-rich MLSLs were collected following enzyme removal *via* filtration. Purification of the product was done by the method of Hita *et al.* (2007).[24] The free fatty acid content of the n-3 PUFAs-rich MLSLs was lowered from 2.4% to 0.11%, determined using the procedure described by Firestone and American Oil Chemists (2011).[25] The purified n-3 PUFAs-rich MLSLs were stored in a nitrogen-filled, sealed amber-colored container stored at −20 °C. The main fatty acids identified in the synthesized MLSLs were CA, DHA, and EPA. The total CA content and its concentration at the *sn*-1,3 positions were 28.72% and 42.26%, respectively. DHA was present at 14.23% in total, with 21.10% located specifically at the *sn*-2 position. Similarly, EPA showed a total content of 16.43%, with 10.14% found at the *sn*-2 position. These MLSLs, enriched with *sn*-1,3 CA and *sn*-2 positioned DHA and EPA, have the potential to offer distinguished health advantages.

2.3. Emulsion preparation of n-3 PUFAs-rich MLSLs

Three distinct formulations were applied following the procedure outlined by Chew *et al.* (2018),[26] with some modifications. These formulations consisted of modified starch:maltodextrin (MS:MD, 2 : 1), gum arabic:maltodextrin (GA:MD, 2 : 1), and mixed gum arabic:modified starch:maltodextrin (GA:MS:MD, 1 : 1 : 1) wall materials (Table 1). Prior to emulsification, MS, MD, and GA were suspended in deionized water using a magnetic stirrer overnight. MLSLs was then gradually added and blended using a fast-moving homogenizer (Ultra-Turrax IKA T18, USA) at 22 000 × *g* for 4 min and then at 25 000 × *g* for 2 min.

2.4. Microencapsulation by spray drying

The method of spray drying was carried out under controlled conditions. A freshly prepared emulsion was introduced into the drying chamber at a flow rate of 0.012 L min^{-1}. The drying air was supplied at a rate of 1350 L min^{-1}, while maintaining the inlet temperature at 190 °C. Under steady-state operation, the outlet temperature was stabilized at 100 ± 5 °C. Atomization was carried out at a constant pressure of 400 kPa with an air flow rate of 40 L min^{-1}. The resulting particles were gathered using the cyclone separator and collection vessel.[27] These operating parameters are commonly used in lab-scale spray drying and can be scaled up in industrial systems, where higher feed rates and airflow can be adjusted while maintaining product quality through optimized thermal control and atomization design.

2.5. Characterization

2.5.1. Microencapsulation yield (MY). The microencapsulation yield obtained through spray drying was expressed as a percentage (%) and determined using the following formula;[28]

$$\mathrm{MY}\ (\%) = \frac{\mathrm{WPC}}{\mathrm{WCA}} \times 100$$

where WPC represents the mass of the collected powder (in grams), and WCA denotes the mass of the carrier agents (in grams).

2.5.2. Determination of microencapsulation efficiency (MEE). The total oil content (TO) of the particles was identified using a cold extraction technique involving an organic solvent. For this, 2.5 grams of the sample powder was placed in a screw-capped glass tube along with 8 mL of distilled water. The mixture was then sonicated in a water bath for 5 minutes at ambient temperature. Subsequently, 10 mL of chloroform and 20 mL of methanol were introduced into the tube, following the protocol originally described by Bligh and Dyer (1959).[29] After the tubes were covered and taped shut, they were manually inverted fifty times. To facilitate phase separation, the tubes were shaken for two more minutes after adding an extra 10 mL of chloroform, and then left undisturbed for thirty minutes. Methanol and water, the top hydrophilic phase, were carefully eliminated. Whatman filter paper no. 1 was used to filter the remaining sample in the lower chloroform phase. A 5 mL aliquot of the filtered solution was then placed in an oven set to 100 °C for one hour in order to thoroughly vaporize the solvent.

Table 1 Formulation details and composition of MLSLs microcapsules prepared with different wall materials (MS:MD, GA:MD, and GA:MS:MD)[a]

	Wall materials			Core material (g/100 g)		
Treatments	MS	MD	GA	MLSLs	Wall to the core ratio	Total solid to the water ratio
MS:MD	66.67 g	66.67 g	—	33.33 g	3 : 1	30 : 70
GA:MD	—	66.67 g	66.67 g	33.33 g	3 : 1	30 : 70
GA:MS:MD	33.33 g	33.33 g	33.33 g	33.33 g	3 : 1	30 : 70

[a] MS: modified starch; MD: maltodextrin; GA: gum arabic; MLSLs: medium- and long-chain structured lipids; wall-to-core ratio is expressed in weight/weight (w/w); total solid-to-water ratio refers to the proportion of total solid content (wall + core material) to the water content in the formulation.

The oil content was calculated by weighing the residue left in the beaker.

The surface oil (SO) was assessed using a method by Bae and Lee (2008).[30] To determine extractable surface oil, 1.5 grams of powder was washed with 15 mL hexane for 2 minutes at room temperature in a screw-cap glass tube. Whatman filter paper no. 1 was used to filter the resultant mixture, and 20 milliliters of hexane were used three times to rinse the powder that had accumulated on the filter. After that, the solvent was evaporated at 60 °C until a constant weight was reached, and the non-encapsulated oil was quantified by the mass difference between the empty flask and the one containing the oil residue.[31]

In order to determine the microencapsulation efficiency (MEE), both determinations (TO and SO) according to the following equation;[30]

$$\mathrm{MEE} = \frac{\mathrm{TO} - \mathrm{SO}}{\mathrm{TO}} \times 100$$

2.5.3. Moisture content and water activity (wa). Gravimetric measurement was employed to ascertain the amount of moisture, involving oven drying at 105 °C until a consistent weight was attained, as shown in equation;[32]

$$\text{Moisture content } (\%) = \frac{\text{wet sample weight (g)} - \text{dry sample weight (g)}}{\text{wet sample weight (g)}} \times 100$$

The microcapsule's water activity powders were evaluated at 25 °C using a water activity meter (Labmaster-aw, Novasina AG, Neuheimstrasse, Switzerland).

2.5.4. Wettability and solubility. Every samples was assessed for wettability by measuring the amount of time (min) required to immerse 1 gram of microcapsule powder in 400 mL of distilled water at 25 °C.[33,34]

Solubility was evaluated following the procedure by Santhalakshmy *et al.* (2015),[35] with some changes. Using a magnetic stirrer, 1 gram of powder was combined and added to 100 mL of distilled water at 25 °C. The solution was then centrifuged for five minutes at 3500 × *g*. Twenty-five milliliters of the supernatant were dried at 105 °C. The following formula was then used to ascertain the microcapsule powders' solubility;

$$\text{Solubility } (\%) = \frac{A}{B} \times 100$$

where *A* and *B* stand for the weight of the powder (g) in the supernatant and the powder (g) in the solution, respectively.

2.5.5. Hygroscopicity. Hygroscopicity of the powdered sample was evaluated following the methodology by Rezende *et al.* (2018).[36] 1 gram of the material was put in a desiccator at 25 °C with a sodium chloride-saturated solution (75.29% relative humidity). The following formula was used to calculate the hygroscopicity after seven days;

$$\text{Hygroscopicity } (\%) = \frac{\mathrm{AM}}{\mathrm{SW}} \times 100$$

where SW indicates the sample's weight (g) and AM stands for the adsorbed moisture.

2.5.6. Bulk density (BD). The sample powders' bulk density (BD) was evaluated using the methods by Saifullah *et al.* (2016).[33] In short, a 10 mL graduated measuring glass cylinder was carefully filled with 2 grams of the powder sample. BD was calculated using the following equation;

$$\mathrm{BD}\ (\mathrm{cm}^3) = \frac{\text{sample weight (g)}}{\text{sample volume } (\mathrm{cm}^3)}$$

2.5.7. Tapped density (TD). Tapped density (TD) was analyzed based on the process by Saifullah *et al.* (2016).[33] A 10 mL graduated cylinder was filled with 2 grams of powder, and then tapped 100 times from a height of 20 cm onto a rubber mat to determine tapped volume. Subsequently, TD was determined using the provided equation;

$$\mathrm{TD}\ (\mathrm{cm}^3) = \frac{\text{sample weight (g)}}{\text{tapped volume } (\mathrm{cm}^3)}$$

2.5.8. Particle density (PD). Particle density (PD) was estimated using the methodology outlined by Santhalakshmy *et al.* (2015).[35] A 10 mL cylinder containing 1 gram of powder was mixed with 5 mL of petroleum ether and stirred for 30 seconds. The walls were rinsed with 2 mL of petroleum ether, and the final volume was recorded to calculate PD using the specified formula;

$$\mathrm{PD}\ (\mathrm{cm}^3) = \frac{\text{sample weight (g)}}{(\text{total volume of petroleum ether and suspended particles } (\mathrm{cm}^3) - 7)}$$

2.5.9. Flowability. The microcapsule powders' flowability was evaluated utilizing Carr's index and the Hausner ratio.[33]

Carr's index (CI), which is based on the TD and BD, was utilized to assess the flowability of microcapsule powders.[35] Using the following equation, the microcapsule powders' CI was computed;

$$\mathrm{CI}\ (\%) = \frac{(\mathrm{TD} - \mathrm{BD})}{\mathrm{TD}} \times 100$$

where BD stands for bulk density and TD for tapped density.

The coherence of the microcapsule powders was assessed through the Hausner ratio (HR), which considers TD and BD.[33] Following equation was applied to calculate the HR for the

microcapsule powders, offering insight into their cohesion properties;

$$\mathrm{HR} = \frac{\mathrm{TD}}{\mathrm{BD}}$$

where BD stands for bulk density and TD for tapped density.

2.5.10. Color. A colorimeter (Hunter Lab Ultra Scan PRO Spectrophotometer, produced by Hunter Associates Laboratory, Inc., Virginia, USA) was used to measure the color of the microcapsule powders. Standard black and white tiles were used to calibrate the equipment prior to measurement. A clear plastic bag containing about 5 grams of microcapsule powder was used to measure the color characteristics [L^* (lightness/darkness), a^* (red/green), and b^* (yellow/blue)] on three randomly chosen surfaces of each sample.[37]

2.5.11. Bulk porosity (BP). The bulk porosity (BP) samples were assessed by following the methodology outlined by Saifullah *et al.* (2016),[33] which based on both PD and TD. The assessment of BP was done using the following equation;

$$\mathrm{BP}\ (\%) = \frac{(\mathrm{PD} - \mathrm{TD})}{\mathrm{PD}} \times 100$$

where PD stands for particle density and TD for tapped density.

2.5.12. Size and zeta potential analysis. A Malvern Zetasizer (Nano ZS, Malvern Instruments Ltd., Worcestershire, U.K.) was used to measure the microcapsule suspensions' particle size and polydispersity index (PDI) at 25 °C and a fixed scattering angle of 90°. 0.5 gram of microcapsule powder was dissolved in 100 mL of deionized water to create around 1 mL of microcapsule suspension was poured into disposable cuvettes for size analysis. Zeta potential was determined using a folded capillary cell, with the results expressed as mean ± SD in millivolts (mV). Each measurement was repeated in triplicate.[38,39]

2.5.13. Crystallinity (X-ray diffraction). The assessment of crystallinity was conducted employing an X-ray diffractometer (D2PHASER, Bruker AXS Co. Ltd., Karlsruhe, Germany),[40] with a scanning range spanning from 5–80° in terms of the diffraction angle (2θ). The obtained software (MDI Jade 6) was used to examine the samples' X-ray diffraction structures, and the following formula was used to determine the relative crystallinity (%);

$$\mathrm{RC}\ (\%) = \frac{\text{sum of total crystalline peak areas}}{\text{sum of total crystalline and amorphous peak areas}} \times 100$$

2.5.14. Fourier transform infrared spectroscopy (FT-IR). FT-IR spectrophotometer (Nicolet iS10, Thermo Fisher Scientific Co. Ltd., Waltham, Massachusetts, USA) was used to identify the chemical structure in accordance with the technique by Hu *et al.* (2018).[41] In a ceramic mortar, the sample powder and KBr powder were combined, and the mixture was then formed into pellets. The samples' FT-IR spectra, which covered a wavelength range of 500–4000 cm^{-1}, were acquired in transmission mode with a resolution of 4 cm^{-1}.

2.5.15. Scanning electron microscopy (SEM). SEM analysis was used to look at the particle morphology (SU 1510, Hitachi Corp., Tokyo, Japan).[34] Double-sided sticky tape was used to attach the powder sample onto a specimen holder, and a thin coating of gold was vacuum-coated on top. The coated samples that had been sputtered were then scanned using a 3 kV accelerating beam voltage.

2.5.16. Oxidative stability under accelerated storage. The stored powder samples for 28 days at 55 °C under accelerated circumstances. The peroxide value (PV) of samples was measured at predetermined intervals of 0, 7, 14, 21, and 28 days.[42]

2.5.17. Statistical analysis. Statistical analysis was performed using SPSS 20.0 and Origin 8.0. ANOVA followed by Duncan's multiple range tests ($p \leq 0.05$) was used to assess significant differences. Experiments were conducted in triplicate, and results are presented as mean ± standard deviation.

3 Results & discussion

3.1. Microencapsulation yield

The microencapsulation yields of MLSLs, as presented in Table 2. These results align well with the standards for drying by Du *et al.* (2014).[43] Especially, the GA:MS:MD formulation showed the highest yield, this may be explained by GA's presence, known for its strong film-forming properties. Comparatively, there were no notable variations ($p \leq 0.05$) between GA:MD and GA:MS:MD formulations, likely due to their shared GA content. On the other hand, the MS:MD formulation recorded the lowest yield, possibly because GA is absent from it.

3.2. Microencapsulation efficiency

Microencapsulation effectiveness serves as an important parameter in validating the efficacy of encapsulation procedures, independent of the technique or primary materials used.[44] Particularly in oil encapsulation, such as through the spray drying process, evaluating microencapsulation efficiency becomes important for estimating product quality. The microencapsulation efficiencies of MS:MD, GA:MD and GA:MS:MD microcapsules are presented in Table 2. Spray drying is recognized for yielding powders with high microencapsulation efficiencies, typically around 90%.[45] All three formulations in this study showed remarkable retention of MLSLs, with microencapsulation efficiencies exceeding 85%. Particularly, GA:MS:MD was the most efficient, closely then GA:MD. These findings suggest that the polysaccharides used (GA and MD) played a significant role in enhancing microencapsulation efficiency. Prior research on refined kenaf (*Hibiscus cannabinus* L.) seed oil microcapsules showed similar outcomes.[26]

3.3. Moisture content and water activity (wa)

Moisture content in microcapsules influences key properties such as water activity, flowability, oxidation, and microbial growth. Excess moisture can compromise storage stability by altering wall materials from a glassy to a rubbery state, potentially causing degradation and core leakage.[32] The moisture content of the microencapsulated MLSLs for the MS:MD, GA:MD and GA:MS:MD formulations is presented in Table 2. In

Table 2 Physicochemical properties of MLSLs microcapsule powders, including microencapsulation yield, microencapsulation efficiency, moisture content, water activity, wettability, solubility, and hygroscopicity[a]

Treatments	MS:MD	GA:MD	GA:MS:MD
Microencapsulation yield (MY%)	81.37 ± 0.35[c]	85.59 ± 0.37[b]	87.77 ± 0.47[a]
Microencapsulation efficiency (MEE%)	83.67 ± 0.56[c]	86.23 ± 0.78[b]	90.11 ± 0.56[a]
Moisture (%)	3.23 ± 0.12[a]	2.48 ± 0.37[b]	1.98 ± 0.21[c]
Water activity	0.29 ± 0.02[a]	0.21 ± 0.03[b]	0.17 ± 0.04[c]
Wettability (min)	13.11 ± 0.89[a]	11.67 ± 0.57[b]	9.27 ± 0.72[c]
Solubility (%)	78.23 ± 0.85[c]	81.87 ± 0.59[b]	87.54 ± 0.63[a]
Hygroscopicity (g/100 g)	7.31 ± 0.46[c]	9.45 ± 0.36[a]	8.16 ± 0.15[b]

[a] MS: modified starch; MD: maltodextrin; GA: gum arabic; MY: microencapsulation yield; MEE: microencapsulation efficiency; water activity: ratio of vapor pressure of the material to pure water; wettability: time (min) for powder to completely wet a surface; hygroscopicity: moisture absorbed from air (g/100 g); the results are presented as means of triplicate ($n = 3$) ± standard deviation (SD). Superscript letters (within a column) indicate significant differences ($p < 0.05$).

the GA:MD and GA:MS:MD formulations, GA caused the moisture content to drop, which made wall formation more efficient. Overall, the moisture percentage of all formulations was less than 4%, which is ideal for powders. For the majority of powders used in the food business, the maximum moisture level that may be accepted is 4%.[46] The water activity values for MS:MD, GA:MD and GA:MS:MD is provided in Table 2. Similarly, in the GA:MD and GA:MS:MD formulations, GA's presence resulted in a drop-in water activity. Maintaining low water activity levels can restrict microbial growth, prevent caking issues, enhance physicochemical stability, and overall improve product acceptability.[26] Powders with water activity levels less than 0.3 are generally thought to have longer shelf lives and are more resistant to microbial development.[46]

3.4. Wettability, solubility and hygroscopicity

Microcapsules' ability to absorb water is indicated by their wettability, which is important for their reconstitution as powder. Better physical qualities for food processing are indicated by a powder's ability to dissolve in water more quickly.[26] The wettability data for each microencapsulated sample is presented in Table 2. It was observed that MS:MD exhibited high a wettability time, while GA:MD and GA:MS:MD had lower wettability times, respectively. These findings suggest that the use of GA lowered the wettability time compared to MS:MD formulation. It was reported that lowering particle size might enhance wettability time, agreeing with the outcomes of the study of Dima *et al.* (2016).[47] The range of wettability time for the microcapsule powders in this study showed a broader range than the previously reported 6–10 min for refined kenaf seed oil microcapsules.[26]

The last stage of particle dissolution is solubility, which is a critical determinant of powder quality for ingredients used in the food industry. Poorly soluble powders might cause problems during processing and financial losses.[48] The solubility results are presented in Table 2.

Hygroscopicity refers to a substance's ability to absorb moisture from the air. This property can cause fat in powders to oxidize, affecting their flow and nutritional value. The MS:MD hygroscopicity was notably lower in comparison to GA:MD and GA:MS:MD (Table 2). Earlier studies indicated that samples with less moisture content tend to show heightened hygroscopicity due to the relationship between moisture absorption and the water concentration gradient between the atmosphere and the powder.[49] The MS:MD had the lowest moisture content and hygroscopicity, which was unexpected. This could be due to the larger size of MS:MD particles, limiting their exposure to air moisture. Moisture absorption in GA:MS:MD may be due to hydroxyl groups in GA and MD, and hydrogen interactions with water molecules. The hygroscopicity of microencapsulated MLSLs in this study was lower than that in previous research using GA as the wall material, such as Gagaita fruit extract (14.8% to 18.8%)[50] and rosemary essential oil (15.9% to 18.9%).[48] Microencapsulated refined kenaf seed oil also showed similar results (7.8% to 10.1%).[26]

3.5. Bulk density, tapped density, particle density, flowability, cohesiveness and bulk porosity

The results for the BD, TD, and PD as well as the CI, HR, and BP of the microencapsulated MLSLs for the MS:MD, GA:MD, and GA:MS:MD formulations are presented in Table 3. The BD values for MS:MD, GA:MD, and GA:MS:MD ranged from 0.24 ± 0.03 to 0.38 ± 0.03 g cm^{-3}, which is within the typical range for powders that are microencapsulated.[31] Higher BD signifies a lessened presence of air within the powder, which might be beneficial in mitigating oxidation of lipids while being stored.[26] Density decreases with increased volume for a fixed mass product. Our study observed a similar trend, as particle size increased, BD decreased. The higher content of solids in GA:MD and GA:MS:MD microencapsulated MLSLs also contributed to increased BD. Comparing with microencapsulated flaxseed oil produced by mixing GA combined with MD produced denser particles when combined with whey protein concentrate (WPC) and MS.[31]

TD indicates the maximum powder weight that a container can hold, which is crucial for powder packing, shipping, and marketing. Making higher TD spray-dried powders has the benefit of requiring less storage containers.[31] In this study, the TD in MS:MD, GA:MD and GA:MS:MD of microencapsulated MLSLs ranged from 0.39 ± 0.02 to 0.53 ± 0.02 g cm^{-3}.

Table 3 Powder flow properties and physicochemical characteristics of MLSLs microcapsule powders, including bulk density (BD), tapped density (TD), particle density (PD), Carr index (CI), Hausner ratio (HR), flowability, particle size, polydispersity index (PDI), and zeta potential[a]

Treatments	MS:MD	GA:MD	GA:MS:MD
Bulk density (g cm^{-3})	0.24 ± 0.03^{c}	0.3 ± 0.02^{b}	0.38 ± 0.03^{a}
Tapped density (g cm^{-3})	0.39 ± 0.02^{c}	0.44 ± 0.03^{b}	0.53 ± 0.02^{a}
Particle density (g cm^{-3})	1.02 ± 0.01^{c}	1.19 ± 0.03^{b}	1.39 ± 0.02^{a}
Bulk porosity (%)	70.04 ± 0.05^{a}	66.31 ± 0.06^{b}	61.88 ± 0.08^{c}
Carr index (%)	38.73 ± 9.92^{a}	31.32 ± 0.77^{b}	27.72 ± 2.04^{c}
Hausner ratio (HR)	1.66 ± 0.27^{a}	1.46 ± 0.02^{b}	1.38 ± 0.04^{c}
Flowability	Awful	Very poor	Poor
Zeta potential (mV)	-21.56 ± 0.06^{a}	-24.31 ± 0.04^{b}	-28.38 ± 0.05^{c}
Particle size (nm)	297.40 ± 2.37^{a}	277.34 ± 0.41^{b}	222.25 ± 4.41^{c}
PDI	0.41 ± 0.01^{a}	0.34 ± 0.05^{b}	0.28 ± 0.03^{c}

[a] MS: modified starch; MD: maltodextrin; GA: gum arabic. The results are presented as means of triplicate ($n = 3$) ± standard deviation (SD). Superscript letters (within a column) indicate significant differences ($p < 0.05$).

GA:MS:MD microencapsulated MLSLs exhibited the highest TD, followed by GA:MD microencapsulated MLSLs. The wall material ratio significantly affects TD. Powder characteristics produced through spray drying with high TD are conducive to storage in smaller containers for convenience. Furthermore, a greater BD suggests that the powders contain less air, which may aid stop fat oxidation while being stored.[31]

Microencapsulated MLSLs' PD varied from 1.02 ± 0.01 to 1.39 ± 0.02 g cm^{-3}. MS:MD microencapsulated MLSLs oil revealed a much lower PD ($p < 0.05$) in contrast to GA:MD and GA:MS:MD microencapsulated MLSLs. The PD of GA:MD and GA:MS:MD microcapsules was found to be similar with the results by de Barros Fernandes *et al.* (2014),[48] who employed GA to microencapsulate (1.0–1.3 g mL^{-1}) of rosemary essential oil.

CI and HR are two interrelated parameters derived empirically, serving as indicators of flow behavior according to tapped and bulk densities.[51] CI assesses the free-flowing characteristic; HR assesses the cohesion of the powder. In this study, CI values indicating poor, very poor and awful flowability (Table 4). HR ranged from 1.38 ± 0.04 to 1.66 ± 0.27 for the developed microencapsulated MLSLs, with higher values suggesting greater cohesion and lower flowability. MS:MD formulation showed awful flowing characteristics, with GA:MD formulation being very poor flowing and GA:MS:MD formulation poor flowing. Poor flowability is indicated by high CI and HR mean values, typically associated with high interparticle friction.[52]

Table 4 Flowability and cohesiveness of MLSLs microcapsule powders, assessed using Carr's index (CI) and Hausner ratio (HR)[a]

Flowability	CI (%)	HR
Excellent	0–10	1.00–1.11
Good	11–15	1.12–1.18
Fair	16–20	1.19–1.25
Passable	21–25	1.26–1.34
Poor	26–31	1.35–1.45
Very poor	32–37	1.46–1.59
Awful	>38	>1.60

[a] CI: Carr's index; HR: Hausner ratio; flowability classification is based on the CI and HR ranges. Source: Lebrun *et al.*[74]

The CI and HR values of the MS:MD and GA:MD microencapsulated MLSLs were considerably lower ($p < 0.05$) for GA:MS:MD, indicating improved flowability facilitated by GA compared to others. However, according to earlier research, flaxseed oil microcapsules had terrible flowability with high CI values (33.7–48.7),[31] sunflower oil[53] and fish oil.[54] With similar mean CI (33.72% to 48.65%) and HR (1.53–1.96) values reported for microencapsulation of flax oil with zein, the microcapsule powders produced in this study were very compressible.[55]

BP is a crucial property in the food industry, particularly concerning the reconstitution of dry powders. It indicates the ratio of the volume of voids between the particles and the volume of pores to the total volume occupied by the powder.[26] According to the research findings, the BP of GA:MS:MD microencapsulated MLSLs differed significantly ($p < 0.05$) from that of GA:MD and MS:MD microencapsulated MLSLs. However, the BP values obtained in this study were lower than those reported by Jinapong *et al.* (2008) for soy milk powders (70% to 74.5%).[56] High BP levels suggest the presence of numerous wipers among particles, which can trap oxygen and lead to degradation reactions.[35]

3.6. Color values

Color parameters, including luminosity L^* [(degree of lightness on a scale of 0–100 from black to white)], a^* [(degree of redness (+) to greenness (−)], and b^* [(degree of yellowness (+) to blueness (−)] are presented in the Table 5.[57] As indicated in Table 5,

Table 5 Color parameters of MLSLs microcapsule powders, indicating the visual characteristics of the formulations[a]

Parameters	L^*	a^*	b^*
MS:MD	94.87 ± 2.02^{a}	-0.73 ± 0.04^{c}	8.78 ± 0.21^{a}
GA:MD	95.02 ± 3.04^{a}	-0.64 ± 0.01^{b}	8.42 ± 0.49^{a}
GA:MS:MD	95.54 ± 2.1^{a}	-0.55 ± 0.02^{a}	7.61 ± 0.38^{b}

[a] MS: modified starch; MD: maltodextrin; GA: gum arabic. Color values are expressed as L^* (lightness), a^* (red-green), and b^* (yellow-blue). Data are shown as mean ± SD ($n = 3$). Different superscript letters in the same column indicate significant differences ($p \leq 0.05$).

no significant differences ($p \leq 0.05$) were observed among the mean values of lightness (L^*) for the microcapsule powder formulations obtained in this study. The L^* values suggesting that all samples tended toward a white color. Mean values of a^* indicating a tendency toward a green color for all samples. Interestingly, the GA:MS:MD formulation showed a significantly lower ($p \leq 0.05$) mean value of a^* compared to other formulations. Mean values of b^* suggesting a tendency toward a yellow color for all samples. Moreover, GA:MS:MD formulation showed a significantly lower ($p \leq 0.05$) mean value of b^* compared to other formulations.

3.7. Size and zeta potential analysis

The particle size of the microcapsule powders showed a significant difference among the three formulations, as presented in Table 3. The GA:MS:MD formulation had the smallest particle size, followed by GA:MD and MS:MD. This trend indicates that the combination of gum arabic, maltodextrin, and modified starch in GA:MS:MD enhances emulsification and spray drying processes, resulting in more compact and homogeneous microcapsules. Similar results were observed by Korma *et al.* (2019),[46] where wall materials like whey protein isolate (WPI) and MD influenced the particle size distribution, producing smaller and more uniform microcapsules due to improved emulsification. Smaller particle sizes are typically associated with improved solubility, dispersion properties, and enhanced bioavailability, crucial for functional food and pharmaceutical applications. The PDI values ranged from 0.28 ± 0.03 (GA:MS:MD) to 0.41 ± 0.01 (MS:MD), as presented in Table 3. A lower PDI value indicates a narrower particle size distribution, meaning the particles are more uniform. GA:MS:MD exhibited the most homogeneous distribution, supporting its enhanced stability and uniformity. The relatively higher PDI in MS:MD suggests variability in particle size due to less effective emulsification or encapsulation, as also demonstrated by Korma *et al.* (2019).[46] This uniform size distribution in GA:MS:MD contributes to its enhanced stability, better reconstitution properties, and effectiveness in protecting the core material. The zeta potential values were negative across all formulations, with GA:MS:MD exhibiting the most negative value, followed by GA:MD and MS:MD, as presented in Table 3. These findings are consistent with the results reported by Nasri *et al.* (2020),[58] who observed higher absolute zeta potential values for microcapsules with enhanced electrostatic stability. The more negative zeta potential in the GA:MS:MD formulation indicates stronger electrostatic repulsion between particles, enhancing the colloidal stability of the microcapsules. This suggests that GA:MS:MD is less prone to aggregation over time, a critical factor for maintaining the integrity of encapsulated bioactive compounds. In contrast, the lower zeta potential in MS:MD may lead to reduced stability and increased aggregation. Overall, the GA:MS:MD formulation demonstrated superior characteristics in terms of particle size, size distribution, and zeta potential, making it the most effective formulation for producing stable microcapsules with enhanced physicochemical properties. This highlights the critical role of wall materials in optimizing encapsulation, with GA contributing to stability, MD enhancing solubility, and modified starch improving structural integrity.

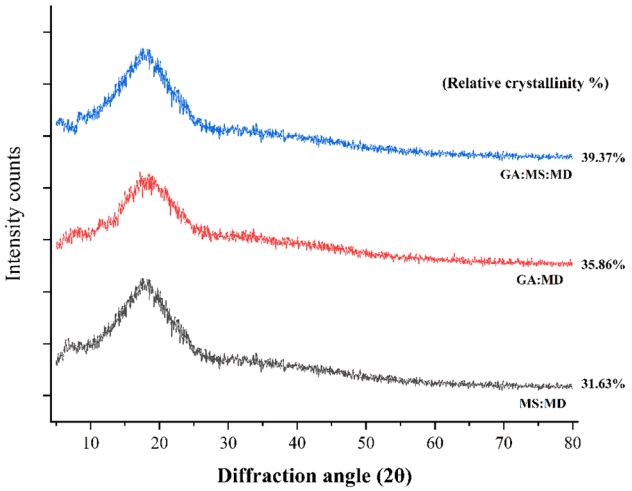

Fig. 1 X-ray diffraction (XRD) patterns of MLSLs microcapsule powders prepared with different wall material formulations (MS:MD, GA:MD, and GA:MS:MD). The GA:MS:MD formulation showed the highest crystallinity, suggesting enhanced structural stability over the others.

3.8. Crystallinity analysis using X-ray diffraction

Determining whether the capsule structures are crystalline or amorphous using XRD analysis is essential for assessing material stability. The diffractograms presented in Fig. 1 illustrate the crystallinity of microencapsulated MLSLs powders. The relative crystallinity shown in GA:MD and MS:MD and GA:MS:MD microencapsulated MLSLs falls within the range of 31.63% to 39.37%. Interestingly, GA:MS:MD microencapsulated MLSLs show the highest relative crystallinity, which is consistent with the findings of the study by Mahdi *et al.* (2020),[34] followed by GA:MD microencapsulated MLSLs. The MS:MD formulation, without GA, shows low crystallization tendency. In contrast, the GA:MS:MD blend exhibits higher crystallinity, indicating better storage stability. However, amorphous samples are hygroscopic and may absorb moisture over time, leading to quality degradation, nutrient loss, structural damage, and microbial instability.[59]

3.9. Structural analysis of microcapsules using Fourier transform infrared spectroscopy (FT-IR)

The properties of MS:MD, GA:MD, and GA:MS:MD microcapsules containing MLSLs were assessed using FT-IR analysis. The spectra of the microcapsules (MS:MD, GA:MD, and GA:MS:MD), fish oil, MLSLs, MS, MD, and GA are shown in Fig. 2. In fish oil and MLSLs, the observed absorbance peaks at 710 and 700 cm^{-1}, and 2852 and 2847 cm^{-1} showed the presence of DHA. Similarly, the broad range of wavelengths from 2925 to 2858 cm^{-1} and 2992 cm^{-1} to 2854 cm^{-1} showed the presence of PUFAs, while wavelengths from 1745 to 1751 cm^{-1} and 1754 to 1759 cm^{-1} indicated ester carbonyl.[60] Furthermore, the 710 and 721 cm^{-1} regions revealed fish oil's content of FAs with *cis*

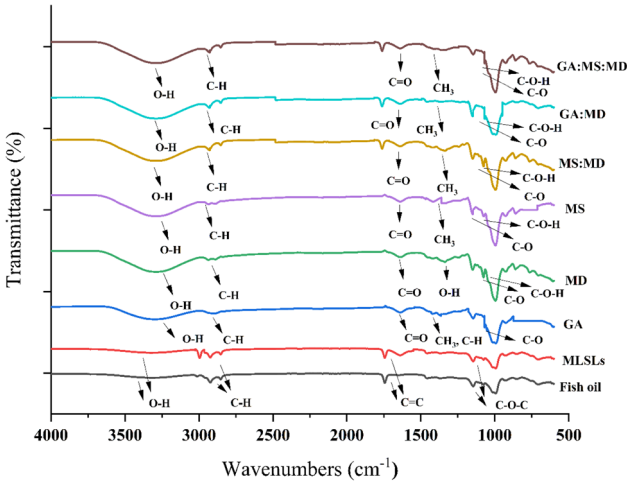

Fig. 2 Fourier Transform Infrared (FT-IR) spectra of raw materials (MS, MD, GA), fish oil, MLSLs, and microcapsules (MS:MD, GA:MD, GA:MS:MD). Key functional groups are labelled. The reduction/disappearance of MLSL peaks (1751, 1149, 2854, and 2992 cm^{-1}) in microcapsules confirms effective encapsulation.

double bonds and MLSLs.[61] In addition, prominent vibrational modes showed by fish oil and MLSLs, including C–H stretching at 2925 to 2858 cm^{-1} and 2992 to 2854 cm^{-1}, respectively. Furthermore, the bands at 1745 and 1751 cm^{-1} and 1754 to 1759 cm^{-1} correspond to C=C stretching, along with a prominent flat stretching at 3429 and 3472 cm^{-1} (O–H stretching). In addition, the bands at 1153 and 1149 cm^{-1} in fish oil and MLSLs corresponding to C–O–C stretching.

The GA spectra showed absorption bands at 3296 cm^{-1} (O–H stretching), 2914 cm^{-1} (C–H stretching, carboxylic group), 1640 cm^{-1} (C=O stretching/N–H bending), 1423 cm^{-1} (CH_3 and C–H bending), and 1015 cm^{-1} (C–O stretching). These results link with those that have been reported by Chew *et al.* (2018).[26] The range of MD revealed absorption bands at several wavelengths, including O–H stretching at 3297 cm^{-1}, C–H stretching from the carboxylic group at 2938 cm^{-1}, C=O stretching at 1636 cm^{-1}, O–H bending at 1332 cm^{-1}, and C–O stretching and C–O–H bending at 1158 cm^{-1}, 1077 cm^{-1}, and 1010 cm^{-1}. These observations align with the published findings by Kang *et al.* (2019).[32] The FT-IR spectra showed that the absorption bands of MS were located at 2941 cm^{-1} (C–H stretching, carboxylic group), 3266 cm^{-1} (O–H stretching), 1648 cm^{-1} (C=O stretching), 1360 cm^{-1} (CH_3 bending), and 1153 cm^{-1}, 1075 cm^{-1}, and 995 cm^{-1} (C–O stretching and C–O–H bending). Similar findings were documented in earlier research by Chew *et al.* (2018).[26]

Notably, the characteristics bands of MLSLs at 1751, 1149, 2854, and 2992 cm^{-1} were significantly reduced in the MS:MD, GA:MD and GA:MS:MD microencapsulated forms, clearly indicating successful encapsulation of the MLSLs.[62] They displayed carboxylic group peaks (C–H stretching) at 2927 cm^{-1} and hydroxyl peaks (O–H stretching) at 3259 cm^{-1}. All formulations showed C–O stretching and C–O–H bending at 1159 cm^{-1}, 1075 cm^{-1}, and 1011 cm^{-1}.[26,34] Additionally, various characteristic peaks associated with GA:MD and GA:MS:MD based microcapsules resembled those of GA. These two formulations contain highest concentrations of GA. Some minor bands within the 650–1250 cm^{-1} range observed in MD were disappeared in the MS:MD, GA:MD and GA:MS:MD microencapsulated MLSLs, implying that GA and MS had integrated MD, and had achieved chemical stability.

3.10. Morphology analysis of microcapsules using scanning electron microscope (SEM)

The SEM analysis of the microencapsulated MLSLs oil powders, as shown in Fig. 3, revealed that the morphology of the microcapsules was not significantly affected by the MS:MD, GA:MD, and GA:MS:MD formulations. Overall, the microencapsulated powders exhibited a variety of sizes and spherical shapes. The spray-dried microcapsules were observed to have a diverse size distribution, consistent with previous findings.[26] Despite the fact that spray-dried particles should normally have a spherical form and range in size from 10 to 100 μm, the microcapsules looked spherical or semi-spherical.[63] Moreover, the purpose of this analysis was to identify any fractures, cracks, or defects that could expose the encapsulated material, potentially leading to oxidation and deterioration.[64] Interestingly, there were no major signs of fissures or cracking on the MS:MD, GA:MD and GA:MS:MD microencapsulated MLSLs, indicating that these wall materials contributed to better retention and stability of the encapsulated products. Although minor shrinkage and surface wrinkles were observed—typically in spray-dried powders—they did not compromise structural integrity or oxidative stability, as reported by Zhang *et al.* (2022).[65] Minor surface imperfections, such as wrinkles, may improve rehydration and dispersibility by increasing surface area and facilitating faster water penetration.[12] Recent reviews further support that controlled morphology variations in spray-dried particles do not adversely affect their functional performance.[66] Furthermore, a few small, hollow, spherical objects were also seen in the powders.[62] These structures can enhance encapsulation by reducing core material migration to the surface and improving dispersibility due to lower density.[67,68] These results are consistent with previous research that used GA as carriers, where SEM examinations frequently showed spherical forms and abnormalities with some shrinkages.[26,50] A rise in the spray dryer's intake temperature, which quickens the droplets' rate of drying, might be the cause of the microcapsules' varying sizes. Some microcapsules showed signs of cracks, fractures, and contractions, most likely as a result of the crust's quick expansion and fast rate of steam generation.[69] Some microcapsules may exhibit shrinkage in the early phases of the spray drying procedure.[70] Variations in drying temperature, droplet size, and feeding ratio throughout the drying procedure may account for the various morphologies and irregular surfaces observed. Shrinkage followed by incipient expansion of the particles may lead to changes in shattered shells and particle size. Thus, such morphological features may contribute positively to functional performance. As a result, the SEM images revealed that the microcapsules had comparable morphological traits, pointing to a consistent drying procedure. The drying process is probably

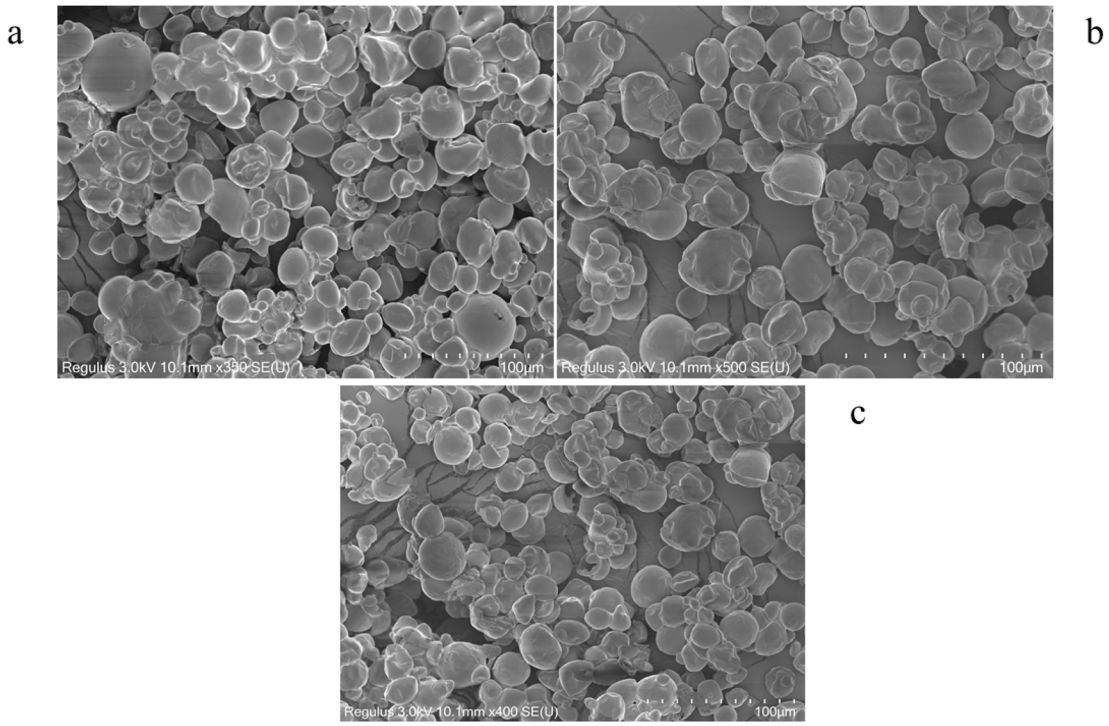

Fig. 3 SEM images of MLSLs microcapsule powders prepared using different wall material formulations: (a) MS:MD, (b) GA:MD, and (c) GA:MS:MD. The GA:MS:MD formulation demonstrates smooth spherical particles with no surface cracks, indicating good physical stability and microencapsulation efficiency. This suggests improved protection against oxidation and other external factors compared to MS:MD and GA:MD formulations.

the cause of the microcapsules that occasionally exhibit surface shrinking.

3.11. Oxidative stability under accelerated storage

Hydroperoxide is the crucial oxidation product found in fats and oils, and it is usually measured using PV.[46] PV growth across seven days intervals in both non-encapsulated MLSLs and microencapsulated forms kept at 55 °C is shown in Fig. 4. Initially, the PV of MLSLs was 0.65 meq O_2 per kg, showing no significant difference compared to microencapsulated oil, which measured 0.75, 0.73, and 0.71 meq O_2 per kg for MS:MD, GA:MD, and GA:MS:MD microcapsules, respectively. These findings suggest that the peroxidation of MLSLs was not negatively impacted by the spray drying technique. In contrast to encapsulated samples, the PV rose more quickly in MLSLs throughout a 14 days storage period. After 14 days, MS:MD and GA:MD microcapsules showed modest increases in PV, whereas GA:MS:MD microcapsules showed no apparent change. The PV of MS:MD and GA:MD microcapsule was 2.56 and 2.39 meq O_2 per kg oil, respectively. After 28 days, whereas the PV of MLSLs reached 6.96 meq O_2 per kg oil. According to these findings, GA:MS:MD microcapsules demonstrated better oxidative stability than both MS:MD and GA:MD microcapsules, which is in line with findings by Premi & Sharma (2017).[71] The increased PV seen in non-encapsulated MLSLs during storage is probably caused by the oxidative breakdown of MLSLs, which produces free radicals (hydroperoxides) during processing and storage. In comparison to other techniques such as freeze-drying and or coacervation, spray drying has been reported to offer better oxidative protection in lipid-based systems due to rapid formation of a protective matrix and lower residual moisture content. For example, coacervation-based systems often result in porous matrices, while freeze-dried powders can retain more oxygen due to longer processing time and high moisture,

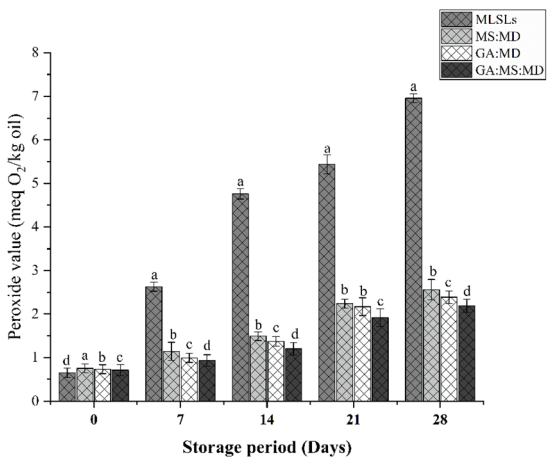

Fig. 4 Peroxide values of microencapsulated MLSLs formulations (MS:MD, GA:MD, and GA:MS:MD) and unencapsulated MLSLs, measured during accelerated storage at 55 °C over 28 days ($n = 3$). Error bars represent the standard deviation (±SD) of triplicate measurements. The GA:MS:MD microcapsules exhibited the lowest peroxide values, indicating superior oxidative stability compared to the MS:MD and GA:MD formulations.

making them more prone to oxidation.[72,73] In conclusion, MLSLs' oxidative stability was enhanced by microencapsulation; the largest improvement was noted when the GA:MS:MD formulation was used.

4 Conclusions

The n-3 PUFAs-rich MLSLs were successfully microencapsulated and spray-dried into powder form using three wall material combinations: MS:MD (2 : 1), GA:MD (2 : 1), and GA:MS:MD (1 : 1 : 1). All formulations produced well-defined microcapsules, as evidenced by SEM-imaging. Among them, the GA:MS:MD formulation emerged as the most effective, exhibiting superior loading efficiency and encapsulation yield, thereby demonstrating the highest retention of the bioactive core material. Additionally, GA:MS:MD microcapsules showed improved bulk, tapped, and particle densities – key indicators of enhanced storage stability.

These microcapsules also exhibited the lowest porosity and fastest wettability, reflecting efficient reconstitution properties. X-ray diffraction analysis confirmed that the GA:MS:MD microcapsules had the highest relativity crystallinity, supporting their enhanced storage stability as compared to the other formulations. FT-IR spectra indicated the absence of core material on the surface, suggesting successful encapsulation across all samples. Furthermore, oxidative stability tests under accelerated storage conditions revealed that the GA:MS:MD formulation offered significantly better protection of the n-3 PUFAs, thereby extending the shelf life of the sensitive oil.

Overall, microencapsulation using the GA:MS:MD combination proved to be a highly effective strategy for developing stable, n-3 PUFAs rich MLSLs microcapsules. These findings support the application of GA:MS:MD microcapsules in functional food and pharmaceuticals products, where long-term stability and oxidative protection are essential.

Data availability

The data supporting the findings of this research are available in the article.

Author contributions

Mudassar Hussain: as the first author, investigation, data extraction, methodology, validation, original manuscript writing, software. Abhishek Bisht: writing – review & editing, visualization. Imad Khan: data analysis, writing – review & editing. Muneeba Naseer Chaudhary: writing – review & editing, visualization. Nida Kanwal: writing – review & editing. Muhammad Umair Khalid: writing – review & editing. Mst Nushrat Yiasmin: writing – review & editing, visualization. Arif Hussain: writing – review & editing. Xiaoqiang Zou: supervision, writing – review & editing, conceptualization, funding acquisition, visualization, investigation.

Conflicts of interest

The authors declare no conflicts of interest.

Acknowledgements

This work was supported by the National Natural Science Foundation of China (31601433).

References

1 U. Nations, *Transforming our World: The 2030 Agenda for Sustainable Development*, United Nations General Assembly, **https://sdgs.un.org/goals**, accessed 01, September, 2015.
2 M. E. da Silva Júnior, M. V. R. L. Araújo, A. C. S. Martins, M. d. S. Lima, F. L. H. Da Silva, A. Converti and M. I. S. Maciel, *Sci. Rep.*, 2023, **13**, 15222.
3 S. Tampucci, G. Tofani, P. Chetoni, M. Di Gangi, A. Mezzetta, V. Paganini, S. Burgalassi, C. S. Pomelli and D. Monti, *Pharmaceutics*, 2022, **14**, 2041.
4 B. Fernandes, M. C. Oliveira, A. C. Marques, R. G. Dos Santos and C. Serrano, *Foods*, 2024, **13**, 3873.
5 Y.-Y. Lee, T.-K. Tang, E.-S. Chan, E.-T. Phuah, O.-M. Lai, C.-P. Tan, Y. Wang, N. A. A. Karim, N. H. M. Dian and J. S. Tan, *Crit. Rev. Food Sci. Nutr.*, 2022, **62**, 4169–4185.
6 M. Yang, J. Zhang, H. Yan, Y. Pan, J. Zhou, H. Zhong, J. Wang, H. Cai, F. Feng and M. Zhao, *Crit. Rev. Food Sci. Nutr.*, 2025, **65**, 2943–2964.
7 M. Hussain, I. Khan, B. Jiang, L. Zheng, Y. Pan, J. Hu, A. Ashraf, A. Din, A. Waleed and A. Khan, *International Journal of Environment, Agriculture and Biotechnology*, 2023, **8**, 94–121.
8 X. Zou, M. Hussain, I. Khan, Y. Wang, B. Jiang, L. Zheng, Y. Pan, J. Hu and A. Ashraf, *Food Biosci.*, 2024, **59**, 104025.
9 X. Zou, I. Khan, Y. Wang, M. Hussain, B. Jiang, L. Zheng, Y. Pan, J. Hu and M. U. Khalid, *Food Chem.*, 2024, **455**, 139907.
10 Y. Wang, W. Wei, Y. Wang, L. Yu, Z. Xing, J. Zhang, Z. Meng and X. Wang, *Compr. Rev. Food Sci. Food Saf.*, 2025, **24**, e70116.
11 I. Khan, M. Hussain, B. Jiang, L. Zheng, Y. Pan, J. Hu, A. Khan, A. Ashraf and X. Zou, *Prog. Lipid Res.*, 2023, **92**, 101255.
12 D. M. Sánchez-Osorno, M. C. López-Jaramillo, A. V. C. Paz, A. L. Villa, M. S. Peresin and J. P. Martínez-Galán, *Pharmaceutics*, 2023, **15**, 1490.
13 M. N. Chaudhary, X. Li, S. Yang, D. Wang, L. Luo, L. Zeng and W. Luo, *Gels*, 2024, **10**, 670.
14 V. G. Hartwig, P. A. P. Cevallos, M. E. Schmalko and L. A. Brumovsky, *Int. J. Food Eng.*, 2014, **10**, 131–138.
15 A. Hussain, M. Hussain, W. Ashraf, K. Ali, A. Hussain, H. M. Phyo, M. U. Khalid, M. Hussain and Z. Lianfu, *Food Biosci.*, 2024, **62**, 105548.
16 S. M. Jafari, E. Assadpoor, Y. He and B. Bhandari, *Dry. Technol.*, 2008, **26**, 816–835.
17 M. C. Otálora, J. G. Carriazo, L. Iturriaga, M. A. Nazareno and C. Osorio, *Food Chem.*, 2015, **187**, 174–181.

18 A. Rehman, S. M. Jafari, Q. Tong, A. Karim, A. A. Mahdi, M. W. Iqbal, R. M. Aadil, A. Ali and M. F. Manzoor, *Int. J. Biol. Macromol.*, 2020, **153**, 697–707.
19 L. Zhao, Q. Tong, H. Wang, Y. Liu, J. Xu and A. Rehman, *Carbohydr. Polym.*, 2020, **250**, 116844.
20 E. Dickinson, *Food Hydrocolloids*, 2003, **17**, 25–39.
21 A. Gharsallaoui, G. Roudaut, O. Chambin, A. Voilley and R. Saurel, *Food Res. Int.*, 2007, **40**, 1107–1121.
22 D. Kanakdande, R. Bhosale and R. S. Singhal, *Carbohydr. Polym.*, 2007, **67**, 536–541.
23 Z. Peng, J. Li, Y. Guan and G. Zhao, *LWT–Food Sci. Technol.*, 2013, **51**, 348–355.
24 E. Hita, A. Robles, B. Camacho, A. Ramírez, L. Esteban, M. J. Jiménez, M. M. Muñío, P. A. González and E. Molina, *Process Biochem.*, 2007, **42**, 415–422.
25 D. Firestone and S. American Oil Chemists, *Official Methods and Recommended Practices of the AOCS*, American Oil Chemists' Society, 6th, 2nd printing edn, 2011.
26 S. C. Chew, C. P. Tan and K. L. Nyam, *J. Food Eng.*, 2018, **237**, 78–85.
27 F. de Melo Ramos, V. S. Júnior and A. S. Prata, *Food Res. Int.*, 2021, **143**, 110283.
28 E. Karrar, A. A. Mahdi, S. Sheth, I. A. M. Ahmed, M. F. Manzoor, W. Wei and X. Wang, *Int. J. Biol. Macromol.*, 2021, **171**, 208–216.
29 E. G. Bligh and W. J. Dyer, *Can. J. Biochem. Physiol.*, 1959, **37**, 911–917.
30 E. Bae and S. J. Lee, *J. Microencapsulation*, 2008, **25**, 549–560.
31 H. C. Carneiro, R. V. Tonon, C. R. Grosso and M. D. Hubinger, *J. Food Eng.*, 2013, **115**, 443–451.
32 Y.-R. Kang, Y.-K. Lee, Y. J. Kim and Y. H. Chang, *Food Chem.*, 2019, **272**, 337–346.
33 M. Saifullah, Y. Yusof, N. Chin and M. Aziz, *Powder Technol.*, 2016, **301**, 396–404.
34 A. A. Mahdi, J. K. Mohammed, W. Al-Ansi, A. D. Ghaleb, Q. A. Al-Maqtari, M. Ma, M. I. Ahmed and H. Wang, *Int. J. Biol. Macromol.*, 2020, **152**, 1125–1134.
35 S. Santhalakshmy, S. J. D. Bosco, S. Francis and M. Sabeena, *Powder Technol.*, 2015, **274**, 37–43.
36 Y. R. R. S. Rezende, J. P. Nogueira and N. Narain, *Food Chem.*, 2018, **254**, 281–291.
37 W. AL-Ansi, A. A. Mahdi, Q. A. Al-Maqtari, M. Fan, L. Wang, Y. Li, H. Qian and H. Zhang, *J. Food Meas. Char.*, 2019, **13**, 2426–2437.
38 S. Ryu, S. Park, H. Y. Lee, H. Lee, C.-W. Cho and J.-S. Baek, *Int. J. Mol. Sci.*, 2021, **22**, 2792.
39 M. U. Khalid, H. M. Phyo, F. Hassan, A. Mushtaq, A. Hussain, M. Hussain, T. Alsulami and W. Yao, *Food Biosci.*, 2024, **62**, 105506.
40 Z. Li, L. Wang, Z. Chen, Q. Yu and W. Feng, *Food Chem.*, 2018, **266**, 551–556.
41 Y. Hu, Y. Li, W. Zhang, G. Kou and Z. Zhou, *Food Hydrocolloids*, 2018, **77**, 588–597.
42 D. Firestone and S. American Oil Chemists, *Official Methods and Recommended Practices of the American Oil Chemists' Society*, American Oil Chemists' Society, 4th, additions and revisions edn, 1990.
43 J. Du, Z.-Z. Ge, Z. Xu, B. Zou, Y. Zhang and C.-M. Li, *Dry. Technol.*, 2014, **32**, 1157–1166.
44 V. B. de Souza, M. Thomazini, M. A. E. Barrientos, C. M. Nalin, R. Ferro-Furtado, M. I. Genovese and C. S. Favaro-Trindade, *Food Hydrocolloids*, 2018, **77**, 297–306.
45 S.-K. Ng, L.-Y. L. Jessie, C.-P. Tan, K. Long and K.-L. Nyam, *J. Am. Oil Chem. Soc.*, 2013, **90**, 1023–1029.
46 S. A. Korma, W. Wei, A. H. Ali, S. M. Abed, L. Zheng, Q. Jin and X. Wang, *Food Res. Int.*, 2019, **116**, 538–547.
47 C. Dima, L. Pătrașcu, A. Cantaragiu, P. Alexe and Ș. Dima, *Food Chem.*, 2016, **195**, 39–48.
48 R. V. d. F. Fernandes, S. V. Borges and D. A. Botrel, *Carbohydr. Polym.*, 2014, **101**, 524–532.
49 R. V. Tonon, C. R. Grosso and M. D. Hubinger, *Food Res. Int.*, 2011, **44**, 282–289.
50 L. D. Daza, A. Fujita, C. S. Fávaro-Trindade, J. N. Rodrigues-Ract, D. Granato and M. I. Genovese, *Food Bioprod. Process.*, 2016, **97**, 20–29.
51 A. Saker, M.-G. Cares-Pacheco, P. Marchal and V. Falk, *Powder Technol.*, 2019, **354**, 52–63.
52 M. Ong, Y. Yusof, M. Aziz, N. Chin and N. M. Amin, *J. Food Eng.*, 2014, **125**, 17–23.
53 C. Turchiuli, M. Fuchs, M. Bohin, M.-E. Cuvelier, C. Ordonnaud, M. Peyrat-Maillard and E. Dumoulin, *Innov. Food Sci. Emerg. Technol.*, 2005, **6**, 29–35.
54 Y. Kagami, S. Sugimura, N. Fujishima, K. Matsuda, T. Kometani and Y. Matsumura, *J. Food Sci.*, 2003, **68**, 2248–2255.
55 S. Quispe-Condori, M. D. Saldaña and F. Temelli, *LWT–Food Sci. Technol.*, 2011, **44**, 1880–1887.
56 N. Jinapong, M. Suphantharika and P. Jamnong, *J. Food Eng.*, 2008, **84**, 194–205.
57 L. Yinbin, L. Wu, M. Weng, B. Tang, P. Lai and J. Chen, *Powder Technol.*, 2018, **340**, 459–464.
58 R. Nasri, W. Taktak, M. Hamdi, N. B. Amor, A. Kabadou, S. Li and M. Nasri, *Mater. Sci. Eng., C*, 2020, **116**, 111164.
59 D. Borrmann, A. P. T. R. Pierucci, S. G. F. Leite and M. H. M. da Rocha Leão, *Food Bioprod. Process.*, 2013, **91**, 23–27.
60 M. Y. Bekhit, B. Grung and S. A. Mjøs, *Appl. Spectrosc.*, 2014, **68**, 1190–1200.
61 P. Karthik and C. Anandharamakrishnan, *Food Bioprocess Technol.*, 2013, **6**, 2780–2790.
62 L. Hu, J. Zhang, Q. Hu, N. Gao, S. Wang, Y. Sun and X. Yang, *J. Drug Delivery Sci. Technol.*, 2016, **36**, 46–54.
63 Z. Fang and B. Bhandari, *Trends Food Sci. Technol.*, 2010, **21**, 510–523.
64 A. Y. Guadarrama-Lezama, L. Dorantes-Alvarez, M. E. Jaramillo-Flores, C. Pérez-Alonso, K. Niranjan, G. F. Gutiérrez-López and L. Alamilla-Beltrán, *J. Food Eng.*, 2012, **112**, 29–37.
65 C. Zhang, W. Zhou, J. Xiang, H. Chen and S. Y. Quek, *J. Food Process. Preserv.*, 2022, **46**, e16950.
66 L. C. da Silva, R. M. Castelo, H. N. Cheng, A. Biswas, R. F. Furtado and C. R. Alves, *Food Technol. Biotechnol.*, 2022, **60**, 308–320.

67 P. Chen, N. Ye, C. He, L. Tang, S. Li, L. Sun and Y. Li, *Appl. Sci.*, 2019, **9**, 228.
68 C. Liang, J. Du, T. Hou, L. Sui, J. Li, Y. Zhao and D. Wu, *Colloid Polym. Sci.*, 2024, **302**, 711–720.
69 M. V. Álvarez-Henao, N. Saavedra, S. Medina, C. J. Cartagena, L. M. Alzate and J. Londoño-Londoño, *Food Chem.*, 2018, **256**, 181–187.
70 R. V. d. F. Fernandes, S. V. Borges, E. K. Silva, Y. F. da Silva, H. J. B. de Souza, E. L. do Carmo, C. R. de Oliveira, M. I. Yoshida and D. A. Botrel, *Ind. Crops Prod.*, 2016, **94**, 413–423.
71 M. Premi and H. Sharma, *Int. J. Biol. Macromol.*, 2017, **105**, 1232–1240.
72 A. Kumar, U. Singh, S. G. Jaiswal, J. Dave, S. Wei and G. G. Hailu, *Sustain. Food Technol.*, 2024, **2**, 1610–1630.
73 A. Michalska-Ciechanowska, J. Brzezowska, P. Nowicka, K. Tkacz, I. P. Turkiewicz, A. Hendrysiak, J. Oszmiański and W. Andlauer, *Molecules*, 2024, **29**, 3586.
74 P. Lebrun, F. Krier, J. Mantanus, H. Grohganz, M. Yang, E. Rozet, B. Boulanger, B. Evrard, J. Rantanen and P. Hubert, *Eur. J. Pharm. Biopharm.*, 2012, **80**, 226–234.